# Reaction Rate Constant Determination of Association Reactions Using Theoretical Calculations: A Case Study of the $HO_2 + NO_2$ Reaction

**Simone Aloisio and Joseph S. Francisco***

*Department of Chemistry and Department of Earth and Atmospheric Sciences, Purdue University, West Lafayette, Indiana 47907*

*Received: February 24, 2000; In Final Form: April 19, 2000*

We have calculated the structure of the complex between $H_2O$ and $HO_2NO_2$. The species $H_2O-HO_2NO_2$ has a relatively large binding energy of 6.5 kcal $mol^{-1}$ at the B3LYP/6−311++G(3df,3pd) level of theory. Vibrational frequencies were also calculated. These data were used to calculate the equilibrium constant for the formation of the complex, as well as the rate constant for its dissociation. Using these calculations in conjunction with the Troe method, we computed a reaction rate constant for the $HO_2-H_2O$ complex with $NO_2$ and compared it to the rate constant for $HO_2 + NO_2$. The $HO_2-HO_2NO_2$ complex is presented for a point of comparison.

## I. Introduction

Pernitric acid (PNA) is an important reservoir species that couples both the $HO_x$ and the $NO_x$ chemical families. This type of coupling is critical to many atmospheric processes, including stratospheric ozone removal.[1] The major production route for pernitric acid is from the radical−radical reaction of the hydroperoxyl radical ($HO_2$) and nitrogen dioxide ($NO_2$) via the reaction[2−12]

$$HO_2 + NO_2 + M \rightleftarrows HO_2NO_2 + M \quad (1)$$

This reaction has also been suggested[13−16] to play an important role in the destruction of $HO_x$ species through the following mechanism.

$$HO_2 + NO_2 + M \rightleftarrows HO_2NO_2 + M \quad (1)$$

$$HO_2NO_2 + OH \rightarrow H_2O + O_2 + NO_2 \quad (2)$$

$$\text{net:} \quad OH + HO_2 \rightarrow H_2O + O_2$$

The enhancement of the rate of reaction 1 by the presence of water can influence the importance of this reaction. Sander and Peterson[17] studied the reaction of $HO_2$ and $NO_2$ in the presence of water vapor and found that the reaction rate is significantly enhanced. It was suggested that the enhancement involves an intermediate formed by the reaction of the hydroperoxyl radical−water complex ($HO_2-H_2O$) with $NO_2$. This intermediate formed by the reaction has been suggested to be more stable with respect to dissociation than the noncomplexed intermediate because of the larger number of vibrational modes available for energy dispersal. In this study, we present the results of our calculations of the probable intermediate formed, the $H_2O-HO_2NO_2$ complex. We calculate the structure, rotational constants, vibrational frequencies, and energetics of this complex. Based on the observed enhancement of the $HO_2 + NO_2$ reaction in the presence of water and the proposed mechanism for the enhancement given by Sander and Peterson,[17] the reaction rate constant for the reaction involving the water-complexed hydroperoxyl radical with nitrogen dioxide should be faster than that for isolated $HO_2$ and $NO_2$. That is, reaction 3 should be faster than reaction 1.

$$HO_2-H_2O + NO_2 + M \rightleftarrows H_2O-HO_2NO_2 + M \quad (3)$$

Because the $HO_2-H_2O$ complex has not been observed in the gas phase, the rate constant for reaction 3 cannot be directly measured experimentally. In the present work, we use density functional theory to estimate salient features of the potential energy surface, using this information to estimate the reaction rate constants for both of these reactions.

## II. Computational Methods

All calculations were performed using the Gaussian 94 suite of programs.[18] Geometries were optimized using the Becke three-parameter hybrid functional combined with the Lee, Yang, and Parr correlation [B3LYP] density functional theory method.[19] This method has been shown to produce reliable results for hydrogen-bonded complexes when compared with other methods.[20,21] Basis sets employed were the 6-31G(d), 6-311++G (d,p), 6-311++G (2d,2p), 6-311++G(2df,2p), and 6-311++G (3df,3pd). Frequency calculations were also performed at the B3LYP/6-311++G(3df,3pd) level of theory. Zero-point energies taken from these frequency calculations can be assumed to be an upper limit because of the anharmonic nature of the potential energy surface. We use the data provided by these calculations to determine the reaction rate constants for reactions 1 and 3. The methods used will be discussed in the following section.

## III. Results and Discussion

**A. Structure and Energy of the Species Studied.** Saxon and Liu[22] and, more recently, Chen and Hamilton[23] have performed theoretical studies of pernitric acid. Chen and Hamilton showed that the B3LYP method calculated a minimum structure similar to that of both Møller−Plessett perturbation theory (MP2) and quadratic configuration interaction theory with single and double substitution (QCISD) using similar size basis sets. Our calculated geometry for PNA is given in Table 1. It is in good agreement with the structure calculated by Chen and Hamilton, as well as with the experimentally derived results of

10.1021/jp000736i CCC: $19.00 
Published on Web 06/14/2000

**TABLE 1: Geometry of Pernitric Acid**

| | B3LYP | | | | | |
|---|---|---|---|---|---|---|
| coordinate[a] | 6-31G(d) | 6-311++G(d,p) | 6-311++G(2d,2p) | 6-311++G(2df,2p) | 6-311++G(3df,3pd) | expt[b] |
| $HO_1$ | 0.978 | 0.972 | 0.970 | 0.970 | 0.970 | 0.965 |
| $O_1O_2$ | 1.404 | 1.399 | 1.401 | 1.397 | 1.396 | |
| $NO_2$ | 1.511 | 1.531 | 1.516 | 1.516 | 1.515 | 1.511 |
| $NO_3$ | 1.198 | 1.189 | 1.190 | 1.187 | 1.186 | |
| $NO_4$ | 1.199 | 1.190 | 1.192 | 1.189 | 1.188 | |
| $HO_1O_2$ | 102.7 | 103.4 | 103.2 | 103.4 | 103.4 | |
| $O_1O_2N$ | 109.1 | 109.6 | 109.6 | 109.7 | 109.6 | 102.9 |
| $O_2NO_3$ | 116.5 | 116.4 | 116.6 | 116.5 | 116.5 | |
| $O_2NO_4$ | 110.1 | 109.9 | 109.9 | 109.9 | 109.9 | |
| $HO_1O_2N$ | 85.4 | 90.3 | 88.1 | 88.1 | 87.5 | 72.8 |
| $O_1O_2NO_3$ | −10.5 | −9.8 | −9.3 | −9.4 | −9.2 | 0.0 |
| $O_1O_2NO_3$ | 171.0 | 171.1 | 171.8 | 171.7 | 171.9 | |

[a] Bond distances are reported in angstroms, bond angles and dihedrals in degrees. [b] Taken from ref 24.

**TABLE 2: Geometry of the Water−Pernitric Acid Complex**

| | B3LYP | | | | |
|---|---|---|---|---|---|
| coordinate[a] | 6-31G(d) | 6-311++G(d,p) | 6-311++G(2d,2p) | 6-311++G(2df,2p) | 6-311++G(3df,3pd) |
| *R* | 1.732 | 1.768 | 1.776 | 1.777 | 1.767 |
| $H_1O_1$ | 0.998 | 0.986 | 0.985 | 0.985 | 0.985 |
| $O_1O_2$ | 1.405 | 1.397 | 1.399 | 1.396 | 1.395 |
| $NO_2$ | 1.482 | 1.509 | 1.495 | 1.494 | 1.493 |
| $NO_3$ | 1.208 | 1.192 | 1.194 | 1.191 | 1.190 |
| $NO_4$ | 1.202 | 1.194 | 1.196 | 1.193 | 1.192 |
| $H_2O_5$ | 0.972 | 0.963 | 0.962 | 0.962 | 0.962 |
| $H_3O_5$ | 0.970 | 0.963 | 0.962 | 0.962 | 0.962 |
| $H_1O_1O_2$ | 102.2 | 102.8 | 102.8 | 103.0 | 103.0 |
| $O_1O_2N$ | 10.1 | 110.1 | 110.1 | 110.2 | 110.2 |
| $O_2NO_3$ | 117.4 | 117.0 | 117.2 | 117.1 | 117.0 |
| $O_2NO_4$ | 111.1 | 110.4 | 110.5 | 110.5 | 110.5 |
| $H_2O_5H_3$ | 105.3 | 106.7 | 106.3 | 106.4 | 106.2 |
| $H_2O_5H_1$ | 96.5 | 119.4 | 111.7 | 112.8 | 112.4 |
| $O_5H_1O_1$ | 161.5 | 173.9 | 173.7 | 173.7 | 174.3 |
| $H_1O_1O_2N$ | 80.1 | 87.3 | 84.6 | 84.5 | 84.0 |
| $O_1O_2NO_3$ | −13.0 | −8.7 | −9.2 | −9.2 | −9.2 |
| $O_1O_2NO_3$ | 169.0 | 172.4 | 172.1 | 172.1 | 172.1 |
| $H_2O_5H_1O_1$ | −1.4 | −41.0 | −9.6 | −10.6 | −7.1 |
| $H_3O_5H_1O_1$ | 109.4 | 100.9 | 116.0 | 117.8 | 120.2 |
| $O_5H_1O_1O_2$ | −74.0 | −48.1 | −71.2 | −70.7 | −72.8 |

[a] Bond distances are reported in Ångstroms, bond angles and dihedrals in degrees.

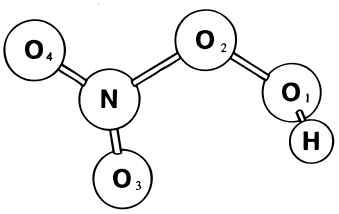


**Figure 1.** Structure of Pernitric Acid.

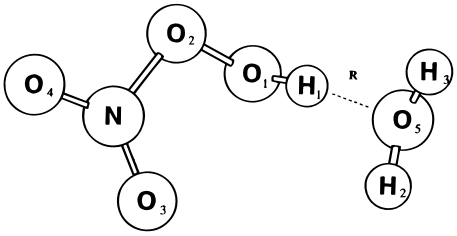


**Figure 2.** Structure of the Water−Pernitric Acid Complex.

Suenram et al.[24] This gives us confidence in the methodology used in this work. The structure of $HO_2NO_2$ is shown in Figure 1.

In this work, we have calculated the structure of the complex between water and pernitric acid, $H_2O-HO_2NO_2$. In this complex, the PNA is a hydrogen donor to the oxygen atom on the water. The structure is shown in Figure 2. The intermolecular bond (*R*) has a calculated distance of 1.767 Å at the B3LYP/6-311++G(3df,3pd) level of theory. This is 0.016 Å shorter than the calculated intermolecular bond in $HO_2-H_2O$,[25] which has similar connectivity, at the same level of theory. The full optimized geometry for this complex is given in Table 2. The oxygen−hydrogen bond in $HO_2NO_2$ is elongated in the water−PNA complex by 0.015 Å, or 1.5%. Whereas the $O_1-O_2$ bond distance is relatively unchanged in PNA, the $N-O_2$ bond distance is decreased by 0.022 Å, about 1.5%. The other coordinates of $HO_2NO_2$ are relatively unchanged.

We have also calculated the structure for the complex between the hydroperoxyl radical and pernitric acid, $HO_2-HO_2NO_2$, shown in Figure 3. In that species, PNA is the hydrogen donor to the terminal oxygen atom of $HO_2$, and the hydroperoxyl radical is a hydrogen donor to one of the oxygen atoms of pernitric acid. These intermolecular bonds, along the $R_1$ and $R_2$ coordinates, have distances of 1.792 and 1.882 Å, respectively. The geometry of the $HO_2-HO_2NO_2$ complex is shown in Table 3. As for the $H_2O-$PNA complex, the $H_1-O_1$ bond is elongated by 1.9%, which is more than in the water−pernitric acid complex. The $N-O_2$ bond is shortened relative to that in isolated PNA by 2.5%, which is more than was the case for $H_2O-HO_2NO_2$. The hydrogen−oxygen bond on the hydroper-

**TABLE 3: Hydroperoxyl Radical−Pernitric Acid Complex**

| | B3LYP | | | | |
|---|---|---|---|---|---|
| coordinate[a] | 6-31G(d) | 6-311++G(d,p) | 6-311++G(2d,2p) | 6-311++G(2df,2p) | 6-311++G(3df,3pd) |
| $R_1$ | 1.798 | 1.843 | 1.811 | 1.817 | 1.792 |
| $R_2$ | 1.901 | 1.926 | 1.909 | 1.913 | 1.882 |
| $H_1O_1$ | 0.996 | 0.987 | 0.987 | 0.987 | 0.988 |
| $O_1O_2$ | 1.405 | 1.398 | 1.399 | 1.396 | 1.394 |
| $NO_2$ | 1.480 | 1.496 | 1.481 | 1.480 | 1.477 |
| $NO_3$ | 1.212 | 1.204 | 1.206 | 1.203 | 1.202 |
| $NO_4$ | 1.197 | 1.187 | 1.189 | 1.186 | 1.186 |
| $H_2O_5$ | 0.994 | 0.986 | 0.986 | 0.986 | 0.986 |
| $O_5O_6$ | 1.326 | 1.322 | 1.323 | 1.320 | 1.318 |
| $H_1O_1O_2$ | 103.0 | 103.7 | 103.6 | 103.8 | 103.8 |
| $O_1O_2N$ | 110.0 | 110.4 | 110.5 | 110.6 | 110.6 |
| $O_2NO_3$ | 117.8 | 117.1 | 117.5 | 117.3 | 117.3 |
| $O_2NO_4$ | 111.1 | 111.2 | 111.2 | 111.2 | 111.3 |
| $H_2O_5O_6$ | 105.5 | 106.1 | 105.8 | 106.0 | 105.9 |
| $O_5O_6H_1$ | 103.2 | 109.4 | 107.0 | 107.5 | 107.2 |
| $O_6H_1O_1$ | 150.9 | 155.3 | 158.1 | 158.0 | 160.1 |
| $H_1O_1O_2N$ | 91.8 | 87.7 | 86.8 | 86.3 | 85.5 |
| $O_1O_2NO_3$ | −9.8 | −11.9 | −11.1 | −11.3 | −11.3 |
| $O_1O_2NO_3$ | 170.6 | 168.9 | 169.7 | 169.5 | 169.5 |
| $H_2O_5O_6H_1$ | 11.3 | 12.5 | 11.8 | 12.0 | 11.6 |
| $O_5O_6H_1O_1$ | 16.0 | 13.2 | 17.2 | 16.9 | 17.9 |
| $O_6H_1O_1O_2$ | −111.9 | −103.3 | −105.7 | −105.5 | −104.0 |

[a] Bond distances are reported in angstroms, bond angles and dihedrals in degrees.

**TABLE 4: Rotational Constants for $H_2O$−PNA and $HO_2$−PNA Complexes**

| | rotational | B3LYP | | | | |
|---|---|---|---|---|---|---|
| species | constant[a] | 6-31G(d) | 6-311++G(d,p) | 6-311++G(2d,2p) | 6-311++G(2df,2p) | 6-311++G(3df,3pd) |
| $H_2O-HO_2NO_2$ | A | 5253 | 5439 | 5430 | 5448 | 5474 |
| | B | 2296 | 1902 | 1953 | 1952 | 1959 |
| | C | 1880 | 1725 | 1737 | 1734 | 1740 |
| $HO_2-HO_2NO_2$ | A | 4580 | 4370 | 4405 | 4418 | 4400 |
| | B | 1530 | 1535 | 1545 | 1543 | 1566 |
| | C | 1269 | 1250 | 1264 | 1261 | 1277 |

[a] Rotational constants are reported in MHz.

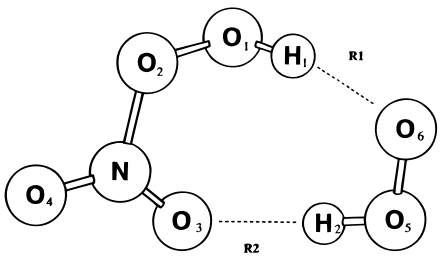


**Figure 3.** Structure of the Hydroperoxyl Radical−Pernitric Acid Complex.

oxyl radical, $H_2-O_5$, is elongated by 1.1% relative to those in isolated $HO_2$. Also, the nitrogen−oxygen bond nearest to the $R_2$ bond on the PNA, $N-O_3$, is elongated by 1.3%. These latter two bonds are indicative of the interaction along $R_2$. The analogous coordinates in $H_2O-HO_2NO_2$ are not significantly different from those in isolated PNA. The rotational constants for both complexes are presented in Table 4.

Pernitric acid has twelve fundamental vibrational modes, and water has three. The water−pernitric acid complex has modes that are similar to these, as well as an additional six new modes that are unique to it. All of these modes are listed in Table 5. The modes that are similar to those of the parent molecules may be shifted with respect to the isolated monomers. The PNA oxygen−hydrogen stretch (mode number 3) is red-shifted by 290 $cm^{-1}$ with respect to that in isolated $HO_2NO_2$. This is consistent with the lengthening of the $H_1-O_1$ bond along that coordinate. This mode also has the largest band intensity, making it a good candidate for experimental detection of this species.

The hydroperoxyl radical−pernitric acid complex also has twenty-one fundamental vibrational modes, listed in Table 6. Many of these modes show shifts similar to those of the $H_2O-HO_2NO_2$ complex. The PNA $H_1-O_1$ stretch (mode number 2) has a larger red shift, 358 $cm^{-1}$, than that in the water−pernitric acid complex. It has weaker intensity, 255.3 km $mol^{-1}$, however. The $H_1$ out-of-plane torsion of PNA (mode number 10) has the same size blue shift, 440 $cm^{-1}$, as that in $H_2O-HO_2NO_2$. Unlike in the water−pernitric acid complex, where modes in common with the water molecule modes are relatively unaffected by complexation, in the $HO_2-HO_2NO_2$ complex, the hydroperoxyl $H_2-O_5$ stretch (mode number 1) is red-shifted by 155 $cm^{-1}$ with respect to the same stretch in isolated $HO_2$. It is also the mode with the largest calculated intensity in $HO_2-HO_2NO_2$, 714.1 km $mol^{-1}$. The hydroperoxyl $H_2-O_5-O_6$ bend is blue-shifted by 87 $cm^{-1}$. Of the intermolecular modes in $HO_2-HO_2NO_2$, the $H_2$ out-of-plane torsion at 523 $cm^{-1}$ is the most strongly absorbing band, with an intensity of 125.2 km $mol^{-1}$.

The binding energies for the $H_2O-HO_2NO_2$ and $HO_2-HO_2NO_2$ complexes are listed in Table 7. At the highest level of theory used, B3LYP/6-311++G(3df,3pd), the binding energies ($D_o$) are calculated to be 6.5 and 6.9 kcal $mol^{-1}$, respectively. There was relatively good convergence as the size of basis set was increased in these calculations. It is clear that the 6-31G(d) basis set is too small to accurately predict energies for these types of molecules, overestimating the binding energies by about 50% for each complex. The complexes have similar binding energies, but for different reasons. In the case of $H_2O-HO_2NO_2$, water is a good hydrogen acceptor, and pernitric acid is

**TABLE 5: Vibrational Frequencies[a] of the Water−Pernitric Acid Complex**

| mode number | mode description | B3LYP/6-311++G(3df,3pd) frequency | shift | intensity |
|---|---|---|---|---|
| 1 | water $H_2-O_5-H_3$ asymmetric stretch | 3902 | −11 | 95.0 |
| 2 | water $H_2-O_5-H_3$ symmetric stretch | 3805 | −9 | 16.2 |
| 3 | PNA $H_1-O_1$ stretch | 3425 | −290 | 766.4 |
| 4 | PNA $O_3-N-O_4$ asymmetric stretch | 1769 | −28 | 424.1 |
| 5 | water $H_2-O_5-H_3$ bend | 1627 | 0 | 66.9 |
| 6 | PNA $H_1-O_1-O_2$ bend | 1549 | +114 | 51.3 |
| 7 | PNA $O_3-N-O_4$ symmetric stretch | 1348 | −5 | 231.0 |
| 8 | PNA $O_1-O_2$ stretch | 1008 | +7 | 36.6 |
| 9 | PNA $N-O_2$ stretch | 846 | +30 | 116.8 |
| 10 | PNA $H_1$ out-of−plane torsion | 814 | +440 | 51.0 |
| 11 | PNA $NO_3$ umbrella | 729 | −21 | 26.1 |
| 12 | PNA $O_3-N-O_4$ bend | 662 | 0 | 3.9 |
| 13 | PNA $O_3-N-O_4$ rock | 474 | +13 | 14.0 |
| 14 | PNA $N-O_2-O_1$ bend | 337 | +29 | 1.3 |
| 15 | intermolecular $H_1-O_5$ stretch | 297 | | 9.5 |
| 16 | intermolecular $H_2$ wag | 274 | | 217.6 |
| 17 | intermolecular $H_2O$ twist | 240 | | 40.8 |
| 18 | PNA $O_2-NO_2$ torsion | 161 | +11 | 5.2 |
| 19 | intermolecular $H_2-O_5-H_1$ bend | 133 | | 46.5 |
| 20 | intermolecular $H_2-O_5-H_1-O_1$ torsion | 56 | | 3.0 |
| 21 | intermolecular $O_5-H_1-O_1-O_2$ torsion | 37 | | 3.4 |

[a] Vibrational frequencies are reported in $cm^{-1}$, intensities in km $mol^{-1}$.

**TABLE 6: Vibrational Frequencies[a] of the Hydroperoxyl Radical−Pernitric Acid Complex**

| mode number | mode description | B3LYP/6-311++G(3df,3pd) frequency | shift | intensity |
|---|---|---|---|---|
| 1 | $HO_2$ $H_2-O_5$ stretch | 3447 | −155 | 714.1 |
| 2 | PNA $H_1-O_1$ stretch | 3357 | −358 | 255.3 |
| 3 | PNA $O_3-N-O_4$ asymmetric stretch | 1756 | −41 | 470.2 |
| 4 | PNA $H_1-O_1-O_2$ bend | 1541 | +106 | 66.1 |
| 5 | $HO_2$ $H_2-O_5-O_6$ bend | 1523 | +87 | 41.1 |
| 6 | PNA $O_3-N-O_4$ symmetric stretch | 1336 | −17 | 204.1 |
| 7 | $HO_2$ $O_5-O_6$ stretch | 1214 | +35 | 12.5 |
| 8 | PNA $O_1-O_2$ stretch | 1009 | +8 | 33.8 |
| 9 | PNA $N-O_2$ stretch | 830 | +14 | 142.4 |
| 10 | PNA $H_1$ out-of−plane torsion | 814 | +440 | 22.4 |
| 11 | PNA $NO_3$ umbrella | 726 | −24 | 19.6 |
| 12 | PNA $O_3-N-O_4$ bend | 657 | −5 | 7.7 |
| 13 | intermolecular $H_2$ out-of−plane torsion | 523 | | 125.2 |
| 14 | PNA $O_3-N-O_4$ rock | 487 | +26 | 12.8 |
| 15 | PNA $N-O_2-O_1$ bend | 341 | +33 | 1.1 |
| 16 | PNA $O_2-O_2$ torsion | 273 | +123 | 37.7 |
| 17 | intermolecular $O_1-H_1-O_6$ bend | 189 | | 25.0 |
| 18 | intermolecular $H_2-O_3$ stretch | 158 | | 4.2 |
| 19 | intermolecular $O_1-H_1-O_6-O_5$ torsion | 119 | | 1.4 |
| 20 | intermolecular $N-O_3-H_2-O_5$ torsion | 81 | | 3.1 |
| 21 | intermolecular $O_2-N-O_3-H_2$ torsion | 55 | | 0.6 |

[a] Vibrational frequencies are reported in $cm^{-1}$, intensities in km $mol^{-1}$.

**TABLE 7: Binding Energies[a] of $H_2O-HO_2NO_2$ and $HO_2-HO_2NO_2$**

| B3LYP basis set | $H_2O-HO_2NO_2$ $D_e$ | $H_2O-HO_2NO_2$ $D_o$ | $HO_2-HO_2NO_2$ $D_e$ | $HO_2-HO_2NO_2$ $D_o$ |
|---|---|---|---|---|
| 6-31G(d) | 12.8 | 10.9 | 12.3 | 10.3 |
| 6-311++G(d,p) | 9.6 | 7.7 | 8.7 | 6.7 |
| 6-311++G(2d,2p) | 8.4 | 6.6 | 8.6 | 6.6 |
| 6-311++G(2df,2p) | 8.4 | 6.5 | 8.5 | 6.5 |
| 6-311++G(3df,3pd) | 8.3 | 6.5 | 8.9 | 6.9 |

[a] Binding energies are reported in kcal $mol^{-1}$.

a good hydrogen donor. The intermolecular bond distance, $R$, is 1.767 Å. In the case of $HO_2-HO_2NO_2$, there are two interactions along the $R_1$ and $R_2$ coordinates. The hydroperoxyl radical is not as good of a hydrogen acceptor as water, as is evident by the longer bond along the $R_1$ coordinate, 1.792 Å. In that case, there is a second interaction in which $HO_2$ is a hydrogen donor to PNA along the $R_2$ coordinate, which has a distance of 1.882 Å. The combination of these two interactions makes the binding energy of the hydroperoxyl radical−pernitric acid complex about 0.4 kcal $mol^{-1}$ larger than that of the water−pernitric acid complex.

Thermodynamic data are listed in Table 8. The data for $HO_2$, $NO_2$, $H_2O$, and PNA were taken from NASA's JPL Publication 97-4.[26] Enthalpy data were extrapolated to other temperatures using Kirchhoff's Law.

$$\Delta H(T_2) - \Delta H(T_1) = \Delta C_p \, \Delta T \qquad (4)$$

where $T$ is the temperature and $\Delta C_p$ is the difference in heat capacity at constant pressure of the substances whose enthalpy is being calculated compared to those of the elements in their natural state. The heat capacities for all of the species at 298 K were taken from the output of the ab initio calculations. Differences in heat capacities were assumed to be independent of temperature. Entropies were extrapolated to different temperatures using the following equation

$$S(T_2) - S(T_1) = C_v \ln(T_2/T_1) \qquad (5)$$

where $C_v$ is the heat capacity at constant volume. The enthalpies of the complexes at zero Kelvin ($\Delta H_f{}^0$) were calculated from the difference in their internal energies and extrapolated to different temperatures using eq 4. Entropies at 300 K were calculated using the ab initio calculations and extrapolated using eq 5.

Using the data in Table 8, we calculated the equilibrium constants for the formation of the complexes ($K_f$) via the following reactions

$$H_2O + HO_2NO_2 \rightleftarrows H_2O-HO_2NO_2 \qquad (6)$$

$$HO_2 + HO_2NO_2 \rightleftarrows HO_2-HO_2NO_2 \qquad (7)$$

At 300 K, $K_f$ is $1.9 \times 10^{-21}$ $cm^3$ $molecule^{-1}$ for $H_2O-HO_2NO_2$ and $6.9 \times 10^{-23}$ $cm^3$ $molecule^{-1}$ for $HO_2-HO_2NO_2$. The difference in $K_f$ between the complexes arises from the change in entropy being much more favorable in the case of the water complex. At 200 K, the formation of the complexes is more favored, with $K_f$ values of $1.3 \times 10^{-19}$ for $H_2O-HO_2NO_2$ and $7.2 \times 10^{-21}$ for $HO_2-HO_2NO_2$.

**B. Determination of Reaction Rate Constants.** As mentioned earlier, Sander and Peterson[17] observed a significant enhancement in the rate constant of reaction 1 in the presence

**TABLE 8: Thermodynamic Data**[a]

| | $HO_2$ | $NO_2$ | $H_2O$ | $HO_2NO_2$ | $HO_2-H_2O$ | $H_2O-HO_2NO_2$ | $HO_2-HO_2NO_2$ |
|---|---|---|---|---|---|---|---|
| $\Delta H_f^0$ | 3.5 | 8.4 | −57.1 | −11.4 | −59.8 | −75.0 | −14.8 |
| $\Delta H_f^{200}$ | 3.0 | 8.1 | −57.7 | −11.8 | −60.4 | −75.8 | −15.7 |
| $\Delta H_f^{300}$ | 2.8 | 7.9 | −57.8 | −12.5 | −60.8 | −76.2 | −16.1 |
| $\Delta S^{200}$ | 51.9 | 54.5 | 42.7 | 64.6 | 65.9 | 79.9 | 80.9 |
| $\Delta S^{300}$ | 54.4 | 57.3 | 45.1 | 70.8 | 72.3 | 90.2 | 91.1 |
| $K_f^{200}$ | | | | | | $1.3 \times 10^{-19}$ | $7.2 \times 10^{-21}$ |
| $K_f^{300}$ | | | | | | $1.9 \times 10^{-21}$ | $6.9 \times 10^{-23}$ |

[a] Enthalpies are reported in kcal mol$^{-1}$, entropies in cal mol$^{-1}$ K$^{-1}$, and equilibrium constants in cm$^3$ molecule$^{-1}$.

of water. This is thought to occur because a complex between water and the hydroperoxyl radical has a faster rate constant in reaction with $NO_2$ than does isolated $HO_2$. It has been proposed that the enhanced rate constant involves the following reaction

$$HO_2-H_2O + NO_2 + M \rightleftarrows H_2O-HO_2NO_2 + M \quad (3)$$

We can use the data in Table 8, in combination with a method first developed by Troe[27,28] and further shown to be effective by Patrick and Golden[29] for reactions of atmospheric importance, to estimate the rate constant for the reverse of reaction 3. We compare this to the reaction rate constant calculated for the formation of pernitric acid not involving complex formation.

$$HO_2 + NO_2 + M \rightleftarrows HO_2NO_2 + M \quad (1)$$

In the method we use, the dissociation rate constant for the complex is calculated using the following equation

$$k_{dissoc} = Z_{LJ}\,\rho(E_0)\,RT(Q_{vib})^{-1}\exp(-E_0R^{-1}T^{-1})\,F_E F_{anh} F_{rot} \quad (8)$$

where $Z_{LJ}$ is the Lennard-Jones collision frequency; $\rho(E_0)$ is the density of states; $R$ is the gas constant; $T$ is the temperature; $Q_{vib}$ is the vibrational partition function for the associated species; $E_0$ is the critical energy; and $F_E$, $F_{anh}$, and $F_{rot}$ are correction terms for the energy dependence of the density of states, for anharmonicity, and for rotation, respectively. The critical energy represents the energy needed for this reaction to take place, in this case the difference in energies between the products and reactants.

To compare our calculated value with a rate that has been measured, we first used this method to calculate the rate constant for reaction 1. The experimentally determined rate constant at 300 K reported in ref 26 is $1.8 \times 10^{-31}$ cm$^6$ molecule$^{-2}$ s$^{-1}$. Our calculated value at the same temperature is $2.2 \times 10^{-32}$ cm$^6$ molecule$^{-2}$ s$^{-1}$. This is the rate constant for the association of $HO_2$ and $NO_2$ in reaction 1 ($k_{assoc}$). Under equilibrium conditions, this is

$$k_{assoc} = K_f k_{dissoc} \quad (9)$$

The calculated value is within an order of magnitude of what is determined experimentally. Differences in experimental and calculated values arise from the fact that we use our calculated energies, which are slightly different from the measured values, to determine the rate constants. We use the calculated numbers to be consistent with the comparison of reactions 1 and 3. For reaction 3, we determine the rate constant to be $4.7 \times 10^{-30}$ cm$^6$ molecule$^{-2}$ s$^{-1}$. This is about 200 times faster than the rate constant we calculated for reaction 1 and about 25 times faster than the experimentally determined rate constant for that reaction. We can appraise these results as the upper and lower limits on the relative rates of reaction 3 and reaction 1. Hence, we estimate the rate constant for reaction 3 to be between $4.7 \times 10^{-30}$ cm$^6$ molecule$^{-2}$ s$^{-1}$ and $3.6 \times 10^{-29}$ cm$^6$ molecule$^{-2}$ s$^{-1}$. The increase in $k_{assoc}$ for reaction 3 compared to that for reaction 1 arises from two contributions: (1) the presence of lower-energy intermolecular vibrational modes in the $H_2O-HO_2NO_2$ complex that contribute to the vibrational partition function ($Q_{vib}$) term in eq 8 and (2) the binding energy of the $H_2O-HO_2NO_2$ complex. For reaction 3, $k_{assoc}$ is about 2 orders of magnitude greater than that for reaction 1.

## IV. Conclusions

We have calculated the structures, energies, and vibrational frequencies for the complexes between water and the hydroperoxyl radical with pernitric acid. The vibrational frequencies reported provide a guide to the experimental detection of these complexes. We use the calculated data to estimate the equilibrium constants for the formation of these complexes. In turn, we use the Troe method to compute the reaction rate constant for the reaction of $HO_2-H_2O$ with $NO_2$. These data support the already-proposed explanation for the enhancement in the rate constant observed in the reaction between $HO_2$ and $NO_2$ in the presence of $H_2O$. These results suggest that the additional stabilization of $HO_2NO_2$ by water may be a driving force for the rate enhancement of the $HO_2 + NO_2$ reaction in the presence of water vapor. The present results are consistent with the results of Sander and Peterson.[17]

**Acknowledgment.** The authors thank the Jet Propulsion Laboratory Supercomputer Center at the California Institute of Technology for ample computational resources to complete this study.

## References and Notes

(1) Wennberg, P. O.; Cohen, R. C.; Stimpfle, R. M.; Koplow, J. P.; Anderson, J. G.; Salawitch, R. J.; Fahay, D. W.; Woodbridge, E. L.; Keim, E. R.; Gao, R. S.; Webster, C. R.; May, R. D.; Toohey, D. W.; Avallone, L. M.; Proffitt, M. H.; Loewenstein, M.; Podolske, J. R.; Chan, K. R.; Wofsy, S. C. *Science* **1994**, *266*, 398.
(2) Simonaitis, R.; Heicklen, J. *J. Phys. Chem.* **1974**, *78*, 653.
(3) Cox, R. A.; Derwent, R. G. *J. Photochem.* **1975**, *4*, 139.
(4) Simonaitis, R.; Heicklen, J. *J. Phys. Chem.* **1976**, *80*, 1.
(5) Niki, H.; Maker, P. D.; Savage, C. M.; Breitenbach, L. P. *Chem. Phys. Lett.* **1977**, *45*, 564.
(6) Hanst, P. L.; Gay, B. W., Jr. *Environ. Sci. Technol.* **1977**, *11*, 1105.
(7) Levine, S. Z.; Uselman, W. M.; Chan, W. H.; Calvert, J. G.; Shaw, J. H. *Chem. Phys. Lett.* **1977**, *48*, 528.
(8) Howard, C. J. *J. Chem. Phys.* **1977**, *67*, 5258.
(9) Graham, R. A.; Winer, A. M.; Pitts, J. N., Jr. *Chem. Phys. Lett.* **1977**, *51*, 215.
(10) Graham, R. A.; Winer, A. M.; Pitts, J. N., Jr. *J. Chem. Phys.* **1978**, *68*, 4505.
(11) Uselman, W. M.; Levine, S. Z.; Chan, W. H.; Calvert, J. G.; Shaw, J. H. *Chem. Phys. Lett.* **1978**, *58*, 437.
(12) Cox, R. A.; Patrick, K. *Int. J. Chem. Kinet.* **1979**, *11*, 635.
(13) Barnes, I.; Bastian, V.; Becker, K. H.; Fink, E. H.; Zabel, F. *Chem. Phys. Lett.* **1981**, *83*, 459.
(14) Trevor, P. L.; Black, G.; Barker, J. R. *J. Phys. Chem.* **1982**, *86*, 1661.
(15) Smith, C. A.; Molina, L. T.; Lamb, J. J.; Molina, M. J. *Int. J. Chem. Kinet.* **1984**, *16*, 41.
(16) Barnes, I.; Bastian, V.; Becker, K. H.; Fink, E. H.; Zabel, F. *Chem. Phys. Lett.* **1986**, *123*, 28.

(17) Sander, S. P.; Peterson, M. E. *J. Phys. Chem.* **1984**, *88*, 1566.
(18) Frisch, M. J.; Trucks, G. W.; Schlegel, H. G.; Gill, P. M. W.; Johnson, B. G.; Robb, M. A.; Cheeseman, J. R.; Keith, T.; Petersson, G. A.; Montgomery, J. A.; Raghavachari, K.; Al-Laham, M. A.; Zakrzewski, V. G.; Ortiz, J. V.; Foresman, J. B.; Cioslowski, J.; Stefanov, B. B.; Nanayakkara, A.; Challacombe, M.; Peng, C. Y.; Ayala, P. Y.; Chen, W.; Wong, M. W.; Andres, J. L.; Replogle, E. S.; Gomperts, R.; Martin, R. L.; Fox, D. J.; Binkley, J. S.; Defrees, D. J.; Baker, J.; Stewart, J. P.; Head-Gordon, M.; Gonzalez, C.; Pople, J. A.; *Gaussian 94*, revision D. 2; Gaussian, Inc.: Pittsburgh, PA, 1995.
(19) Becke, A. M. *J. Chem. Phys.* **1993**, *98*, 5648.
(20) Kim, K.; Jordan, K. D. *J. Phys. Chem.* **1994**, *98*, 10089.
(21) Novoa, J. J.; Sosa, C. *J. Phys. Chem.* **1995**, *99*, 15837.
(22) Saxon, R. P.; Liu, B. *J. Phys. Chem.* **1985**, *89*, 1227.
(23) Chen, Z.; Hamilton, T. P. *J. Phys. Chem.* **1996**, *100*, 15731.
(24) Suenram, R. D.; Lovas, F. J.; Pickett, H. M. *J. Mol. Spectrosc.* **1986**, *116*, 406.
(25) Aloisio, S.; Francisco, J. S. *J. Phys. Chem.* **1998**, *102*, 1899.
(26) DeMore, W. B.; Sander, S. P.; Golden, D. M.; Hampson, R. F.; Kurylo, M. J.; Howard, C. J.; Ravishankara, A. R.; Kolb, C. E.; Molina, M. J.; *Chemical Kinetics and Photochemical Data for Use in Stratospheric Modelling*; Evaluation No. 12; National Aeronautics and Space Administration, Jet Propulsion Laboratory: Pasadena, CA, 1997.
(27) Troe, J. *J. Chem. Phys.* **1977**, *66*, 4745.
(28) Troe, J. *J. Chem. Phys.* **1977**, 66, 4758.
(29) Patrick, R.; Golden, D. M. *Int. J. Chem. Kinet.* **1983**, *15*, 1189−1227.